Differential, integral, and momentum-transfer cross sections for elastic electron scattering by neon: 5 to 100 eV

D. F. Register and S. Trajmar
Jet Propulsion Laboratory, California Institute of Technology, Pasadena, California 91109
(Received 31 January 1983)

Relative elastic-scattering differential cross sections were measured in the 5—100-eV impact energy and 10°—145° angular ranges. Normalization of these cross sections was achieved by utilizing accurate total electron-scattering cross sections. A phase-shift analysis of the angular distributions in terms of real phase shifts has been carried out. From the differential cross sections we obtained momentum-transfer cross sections and established the value of the critical energy and angle (associated with the lowest value of the differential cross section) as 62.5±2.5 eV and 101.7°±1.5°, respectively. The present phase shifts, the critical parameters, and differential, integral, and momentum-transfer cross sections are compared to previous experimental and theoretical results. The error associated with the present data is about 10%.

I. INTRODUCTION

A large number of measurements and calculations have been carried out concerning elastic electron scattering by Ne. The investigations extend from a few hundredths of an eV to a few thousand eV and include differential, integral, and momentum-transfer cross sections. Recent summaries of the available data in the energy region of interest here have been published by O'Malley and Crompton,[1] de Heer *et al.*,[2] Fon and Berrington,[3] and Thirumalai and Truhlar.[4]

Total electron-scattering cross sections (σ_{TOT}) measured at impact energies below the first inelastic threshold represent integral elastic cross sections (σ_{ELA}). Because of the high accuracy of these cross sections, they can be used to calibrate differential cross sections (DCS) and to check the overall consistency of cross-section data. The most recent total cross-section data were obtained by Wagenaar and de Heer,[5] Kauppila *et al.*,[6] Nickel *et al.*,[7] and Wilson[8] and agree among each other to within about 3%. Momentum-transfer cross sections σ^M_{ELA} were determined by O'Malley and Crompton[1] at low energies, by Andrick[9] at intermediate energies, and Gupta and Rees[10] at impact energies of 150 eV and higher. Elastic-scattering phase shifts (η_e) have been obtained experimentally by Andrick[9] and more recently by Williams[11] and Brewer *et al.*[12] Theoretical phase shifts have been calculated by Fon and Berrington[3] and Thirumalai and Truhlar.[4] The critical values of impact energy and scattering angle (deepest minimum in the differential elastic-scattering cross section) was recently measured by Kollath and Lucas,[13] and Beaty *et al.*[14] For further discussion of this question see Refs. 13 and 15.

The present work is the second part of a systematic effort to generate accurate electron-scattering cross-section data at intermediate energies for the rare gases. The approach is similar to the one applied in our first paper for He.[16] Relative differential cross sections (DCS) were measured at 5-, 10-, 15-, 20-, 30-, 50-, 60-, 65-, 70-, 80-, and 100-eV impact energies (E_0) at scattering angles (θ) ranging from 10° to 145°. From these angular distributions real s, p, d, and f phase shifts and integral and momentum-transfer cross sections were obtained. The normalization to the absolute scale was achieved by using a set of integral elastic cross sections derived from total scattering, ionization, and excitation cross-section data. The critical minimum for neon was deduced by interpolation of the measured DCS behavior. A comparison and cross check between the normalization method applied here and the normalization by relative flow techniques will be discussed by one of us (D.F.R.) in a subsequent paper.

II. EXPERIMENTAL METHODS AND PROCEDURES

The elastic-scattering angular distributions were measured by an apparatus described earlier.[16] A collimated Ne beam was crossed by an energy selected electron beam and the elastic-scattering intensity at fixed impact energies was measured over the experimentally accessible range of scattering angles ($-40°$ to $+145°$). The detector consisted of two angle defining apertures, a retarding grid structure, and a channeltron electron multiplier. The elastic-scattering intensities were obtained by scanning the signal as a function of time with a multichannel scaler over a fixed time interval and adding up the counts from all channels corresponding to this time interval. The angular distributions were measured a minimum of three times and an average curve was obtained at each impact energy. For each measurement, the intensity was properly corrected for background gas effects and uv photons as described in Ref. 16.

The Ne beam was generated by a small capillary array and further collimated by a skimmer. With this type of scattering arrangement no effective path length correction was needed in the angular range of the present measurements.[17] Thus, the intensity distribution was equivalent to the relative differential cross sections.

The relative cross-section curves were least-square fitted to an analytical expression representing a partial-wave ex-

pansion with real phase shifts in a manner discussed in Ref. 16. At impact energies below the first inelastic threshold (5, 10, and 15 eV) this analysis could also achieve the normalization to the absolute scale. At the higher impact energies, these parameters are useful to extrapolate the DCS to 0° and 180° for obtaining elastic integral and momentum-transfer cross sections. In the present case the normalization of the data to the absolute scale was, however, based at all impact energies on a set of semiempirical integral elastic cross sections obtained by the procedure discussed for the case of He by Register *et al.*[16] This procedure utilizes total electron-scattering, ionization, and overall electronic-excitation cross sections and the relation $\sigma_{ELA}=\sigma_{TOT}-\sigma_{ION}-\sigma_{EXC}$ (where $\sigma_{EXC}=\sum_n \sigma_n$ and σ_n refers to the integral cross section for the excitation of the nth discrete electronic state). The four recent sets of total electron-scattering cross sections[5–8] and their average values and estimated errors are given in Table I. The ionization (σ_{ION}) and overall electronic-excitation cross sections (σ_{EXC}), their averages, and the associated errors (obtained from Refs. 2 and 18–20) are listed in Table II. The integral elastic cross sections obtained from Tables I and II are given in Table III (column 2). An overview of the integral and total electron-scattering data is shown in Fig. 1.

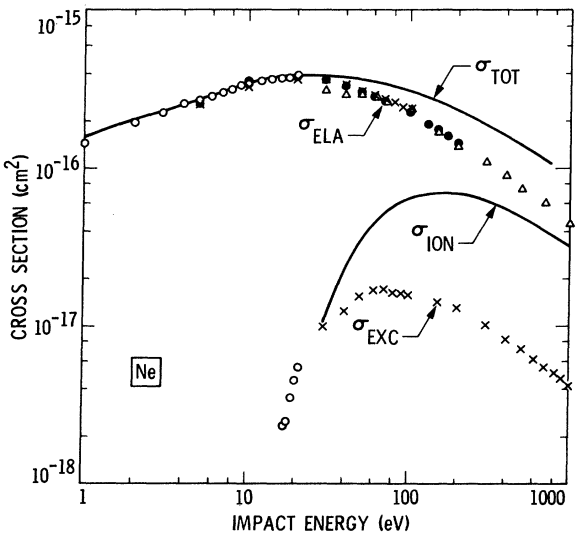

FIG. 1. An overview of the integral and total electron-scattering cross section data. σ_{TOT}: solid line was drawn on the basis of the average data presented in Table I and the data of Refs. 1 and 8 (at low energies). σ_{ELA}: ○, Ref. 9; Δ, Ref. 2; ●, Ref. 3; ×, present. σ_{EXC}: ○, Ref. 19; ×, Ref. 2.

III. RESULTS AND DISCUSSION

A. Phase shifts

Table IV contains the phase shifts obtained by fitting the present angular distributions at the four lowest impact energies. For the purpose of comparison, the phase-shift results of Andrick,[9] Williams,[11] Brewer *et al.*,[12] Fon and Berrington,[3] and Thirumalai and Truhlar[4] are also given.

The iteration procedure used in Ref. 16 was found to be slowly convergent and a reasonably broad range of s-wave phase shifts yielded good χ^2 fits. Therefore, a modified fitting technique was used in which the $l=1$, 2, and 3 phases were obtained as before but the s-wave phase shift was calculated using the $l>0$ phases and the constraint that the integral elastic cross section should equal that of Table III. This s phase shift was then used to reiterate the higher partial waves and the process repeated until satisfactory convergence (one part in 10^6) was obtained. The resulting s-wave phase shift was found to lie approximately in the center of the range of values obtained by the technique of Ref. 16 while for $l>0$ the values changed by less than 2%. This constraint on the s wave caused a few percent change in the fitted phase shifts and differential cross sections compared with the unconstrained solutions. For purposes of comparison the integral elastic cross sections obtained by the latter calculation are given in column 3 of Table III. Below inelastic threshold energies the discrepancy between the unconstrained phase-shift-derived integral cross sections and the more accurate semiempirical results is due to the relatively featureless nature of the DCS curves. This causes some ambiguity in the phase shift fitting and causes difficulty in determining the actual zero scattering angle (based on the symmetry of

TABLE I. Total electron-scattering cross sections for Ne.

	σ_{TOT}					
E_0 (eV)	Reference 8	Reference 6	Reference 5	Reference 7	Average	% Error
5	2.68				2.68	3
10	3.25				3.25	3
15	3.55				3.55	3
20	3.65	3.73			3.67	3
30		3.76	3.84	3.90	3.82	3
40			3.76	3.84	3.80	3
50		3.60	3.66	3.71	3.64	3
60			3.56	3.63	3.60	3
65					(3.56)[a]	3
70			3.45	3.59	3.52	3
80			3.33	3.38	3.35	3
90			3.21	3.24	3.22	3
100		3.00	3.09	3.11	3.06	3

[a]Number in parentheses was obtained by interpolation.

TABLE II. Total ionization and excitation cross sections for Ne.

	σ_{ION} 10^{-17} cm^2			σ_{EXC} 10^{-17} cm^2	
E_0 (eV)	Reference 18	Reference 2	Average	Reference 2	Reference 20
20			(0.10)[a]	(0.46)[a]	
30	1.03	1.11	1.07 [5.0][b]	1.00 [20][b]	>1.77
40	2.30	2.42	2.36 [4.6][b]	1.35 [19][b]	
50	3.41	3.60	3.51 [4.3][b]	1.59 [17][b]	>2.05
60	4.40	4.58	4.49 [4.0][b]	1.70 [15][b]	
70	5.19	5.38	5.29 [4.4][b]	1.70 [14][b]	
80	5.83	5.93	6.88 [4.6][b]	1.66 [11][b]	
90	6.35	6.36	6.36 [4.9][b]	1.62 [10][b]	
100	6.74	6.59	6.67 [4.9][b]	1.59 [8][b]	>1.15

[a]Numbers in parentheses were obtained by extrapolation from Fig. 1.
[b]Estimated percentage errors are in square brackets.

scattering around nominal zero angle). At impact energies greater than inelastic threshold, the deviation between column 2 and 3 of Table III is due to the neglect of the inelastic channels (using real instead of complex phase shifts). This forces all the flux into the elastic channel and results in a higher than correct value for the elastic cross section.

In Table IV, the low-energy phase shifts (from the s-wave constrained solutions) are compared with the results of other experimental investigations[9,11,12] the R-matrix calculations of Fon and Berrington,[3] and the model potential calculation of Thirumalai and Truhlar.[4] The conclusions concerning the comparison of experimental results with the calculations of Fon and Berrington can be summarized as follows. For the s wave, the difference beween experiment and theory is nowhere greater than 3%. Since the experimental data all agree within this range, this may be considered a practical limit on the error in the s-wave phase shift. For the P wave the agreement between experiment and theory is typically better than 7% while the agreement among the experiments is approximately 5% (excepting Andrick's P wave at 5 eV). Interestingly, the measured data are systematically higher than theory but still well within any reasonable error estimate associated with this partial wave. For $l>1$ the discrepancies and errors associated with the experimental phase shifts increase dramatically due to their small values. In general, however, the agreement is better at higher energies and appears to be on the order of 10% for $l=2$ and 15–20% for $l=3$. Since the values derived for the $l=3$ phase shifts are quite small, these large errors have little effect on the DCS or integral cross section values.

Thirumalai and Truhlar used simple model potentials in their calculations. We compared our results with theirs for the SEPna potential below inelastic threshold and

TABLE III. Integral elastic cross sections for Ne.

	Present			Theory	
	Semiempirical	From unconstrained phase shifts	% Deviation $\frac{\lvert\sigma_{ELAS}-\sigma_{PS}\rvert}{\sigma_{ELAS}}100$	Fon-Berrington	Thirumalai-Truhlar
E_0 (eV)	(σ_{ELAS})[a] (10^{-16} cm^2)	(σ_{PS}) (10^{-16} cm^2)	(10^{-16} cm^2)	Ref. 3	Ref. 4[b]
5	2.68 [3]	2.32	13	2.67	
10	3.25 [3]	3.65	12	3.50	3.84
15	3.55 [3]	3.68	4		
20	3.61 [3]	3.73	3	3.77	
30	3.61 [4]	3.75	4	3.56	3.64
40	3.43 [4]			3.31	
50	3.13 [5]	3.58	14	3.09	2.73
60	2.98 [5]	4.18	40	2.85	
65	(2.90) [6]	4.06	40		
70	2.82 [6]	3.91	39	2.70	
80	2.60 [6]	3.22	24		
90	2.42 [7]				
100	2.23 [7]	2.83	27	2.25	1.66

[a]Number in parentheses was obtained by interpolation and the numbers in square brackets refer to percentage errors.
[b]SEPna model potential at 10 eV; SEPnaA_1 potential at the other energies.

TABLE IV. Elastic phase shifts for Ne.

E_0 (eV)	Reference	Phase shift (deg) $l=0$	$l=1$	$l=2$	$l=3$
5	Andrick[a]	−29.69	−6.10	2.06	0.57
	Williams (4.90 eV)[b]	−29.97	−4.98	1.55	
	Brewer *et al.*[c]				
	Fon-Berrington[d]	−29.45	−5.10		
	Present	−29.91	−5.22	1.97	0.40
10	Andrick	−45.73	−13.38	5.01	1.13
	Williams	−45.84	−12.61	4.35	
	Brewer *et al.*	−46.15	−13.41	5.01	
	Fon-Berrington	−45.84	−12.43		
	Thirumalai and Truhlar[e]	−47.83	−15.56	4.63	0.98
	Present	−45.08	−12.62	4.51	1.09
15	Andrick	−57.48	−14.46	8.54	1.70
	Williams	−56.84	−18.79	7.85	
	Brewer *et al.*	−54.54	−18.57	7.82	1.28
	Fon-Berrington	−56.84	−18.45		
	Present	−57.08	18.70	7.77	1.66
20	Andrick	−66.65	−24.60	12.03	2.27
	Williams	−65.32	−24.24	11.23	
	Brewer *et al.*	−66.65	−24.61	11.78	2.33
	Fon-Berrington (19.6 eV)	−67.32	−22.98	12.15	2.18
	Present	−65.77	−23.68	10.94	1.99

[a]Reference 9.
[b]Reference 11.
[c]Reference 12.
[d]Reference 3.
[e]Reference 4, SEPna model potential.

SEPnaA$_1$ potential above inelastic threshold. [S, E, Pna, and A$_1$ refer to the static (Hartree-Fock), exchange (semiclassical), nonadiabatic polarization, and phenomenological absorption potential terms, respectively.] The 10-eV phase shifts calculated by Thirumalai and Truhlar differ from the present data by about 10%.

B. Differential cross sections (DCS)

The normalized DCS values are given in Table V and are compared with previous results at 5, 10, 20, and 100 eV in Figs. 2–6. At the lower impact energies (at and below 20 eV) the present results are in excellent (within a few percent) agreement with the experimental measurements of Andrick[9] and Williams and Crowe[21] as well as with the theoretical calculations of Fon and Berrington[3] and Thirumalai and Truhlar.[4] Deviations of the order of 10% do occur occasionally (e.g., 5 eV, the high-angle data of Andrick,[9] or 20 eV, the low-angle data of Williams and Crowe[21]). It should be noted that the phase shifts given by Williams[11] at 20 eV yield low-angle DCS values in ex-

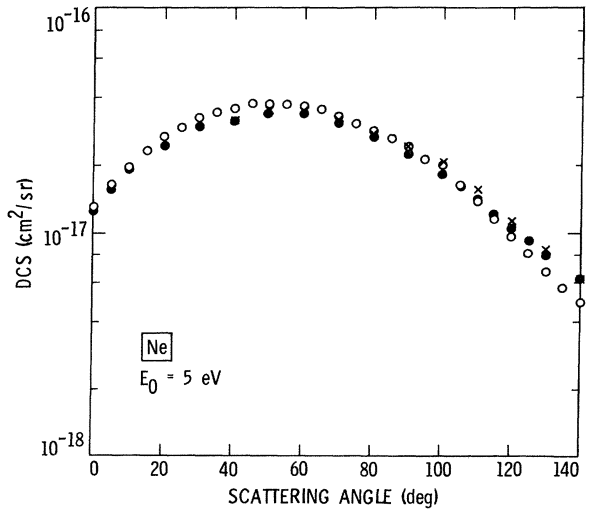

FIG. 2. Elastic differential cross sections at 5 eV: ○, Ref. 9; ●, Ref. 3; ×, present.

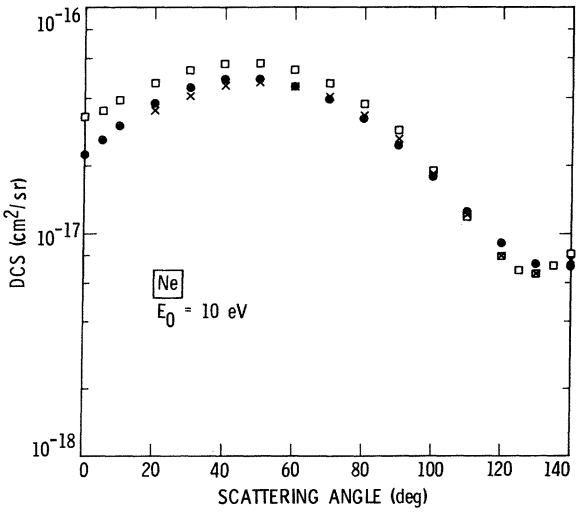

FIG. 3. Elastic differential cross sections at 10 eV: ●, Ref. 3; □, Ref. 4; ×, present.

TABLE V. Elastic differential cross sections (10^{-16} cm^2/sr) for Ne.

θ (deg) \ E_0 (eV)	5	10	15	20	30	50	60	65	70	80	100
10							2.039	2.231	2.212	2.011	2.130
15					0.670	1.171	1.532	1.653	1.624	1.479	1.473
20		0.352			0.611	0.907	1.209	1.257	1.197	1.100	1.036
25			0.412	0.452	0.563	0.729				0.805	0.744
30	0.298	0.400	0.442	0.467	0.514	0.588	0.692	0.701	0.671	0.590	0.516
40	0.332	0.452	0.479	0.480	0.471	0.411	0.450	0.435	0.399	0.335	0.271
50	0.343	0.470	0.503	0.487	0.439	0.319	0.292	0.291	0.252	0.206	0.155
60	0.338	0.449	0.484	0.462	0.388	0.249	0.218	0.193	0.175	0.131	0.0906
70	0.318	0.404	0.429	0.404	0.333	0.180	0.155	0.132	0.1151	0.0831	0.0558
80	0.282	0.336	0.350	0.312	0.244	0.112	0.080	0.075	0.0608	0.0430	0.0279
85							0.0612	0.0426	0.0388	0.0280	0.0200
90	0.246	0.258	0.261	0.220	0.150	0.047	0.0300	0.0223	0.0219	0.0144	0.0117
93											0.0094
94										0.0075	
95						0.0234	0.0113	0.0075	0.0077		0.0094
96										0.0050	
97											0.0091
98										0.0040	
99											0.0091
100	0.199	0.181	0.168	0.134	0.073	0.0098	0.0023	0.00074	0.00221	0.0032	0.0109
101							0.0011	0.00031	0.00140		
102							0.00068	0.00043	0.00102	0.0036	
103						0.0042	0.00033	0.00158	0.00124		
104							0.00090	0.00275	0.00206	0.0057	
105				0.102	0.051	0.0057	0.00183	0.00441	0.00374		0.0167
107						0.0071					
110	0.154	0.121	0.102	0.078	0.041	0.015	0.0141	0.0181	0.0133	0.0179	0.0279
115			0.087	0.065	0.046	0.042	0.0394	0.0447	0.0343	0.0380	
120	0.110	0.080	0.074	0.068	0.064	0.075	0.0770	0.0803	0.0651	0.0651	0.0641
125			0.077	0.080	0.097						
130	0.083	0.068	0.086	0.104	0.142	0.180	0.187	0.170	0.148	0.139	0.117
135											0.162
140	0.063	0.075	0.131	0.183	0.277	0.309	0.252	0.236	0.236	0.235	0.196
145					0.326	0.368				0.270	0.253
% Error	7	7	7	7	8	11	12	12	12	12	13

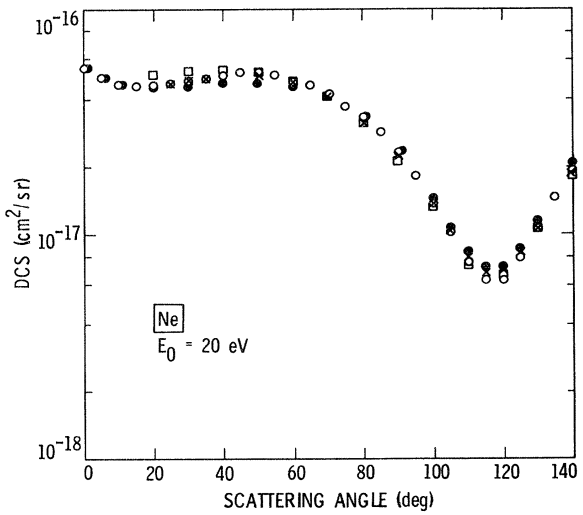

FIG. 4. Elastic differential cross sections at 20 eV: □, Ref. 21; ○, Ref. 9; ●, Ref. 3; ×, present.

cellent agreement with the present data. The cross sections calculated by Thirumalai and Truhlar are about 20% higher than the present results at low angles for 10-eV impact energy. At higher impact energies more data are available.[10,20,22–25] A comparison of the present results at 100-eV impact energy with other experimental and theoretical results are shown in Figs. 5 and 6, respectively. The experimental results agree with each other within about 15%, in general, but deviations on the order of 25% occur at low and high angles and near the DCS minimum. The low-angle data of Jansen *et al.* (5° to 60°) and the Williams and Crowe results at this energy are both in very good agreement with the present data. The theoretical results of Fon and Berrington are in excellent agreement with the present data except at low angles. Apparently some theoretical improvements in treating the long-range interactions would be desirable. A similar comment applies to the results of Thirumalai and Truhlar at low angles and, in addition, their results are lower than the present ones by about 20% at all scattering angles. (Again

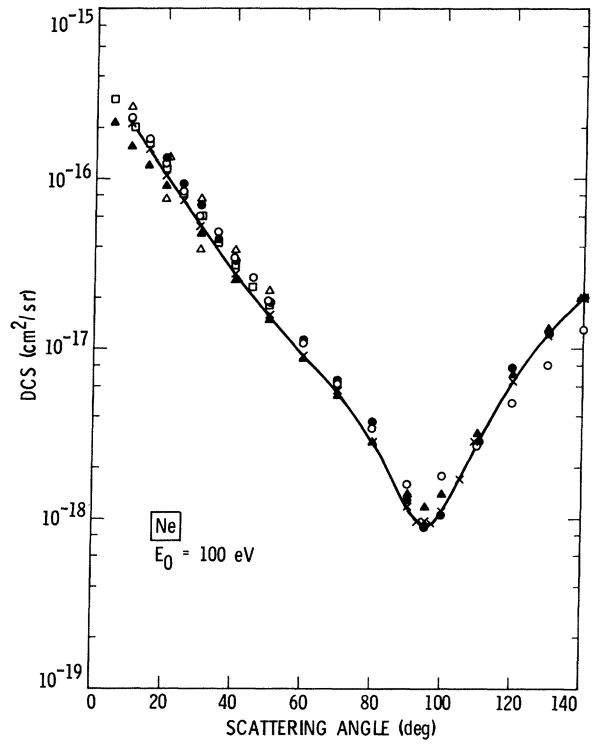

FIG. 5. Comparison of experimental elastic differential cross sections at 100 eV: △, Ref. 22; □, Ref. 23; ○, Ref. 10; △, Ref. 24; ●, Ref. 21; ×, present (connected by solid line).

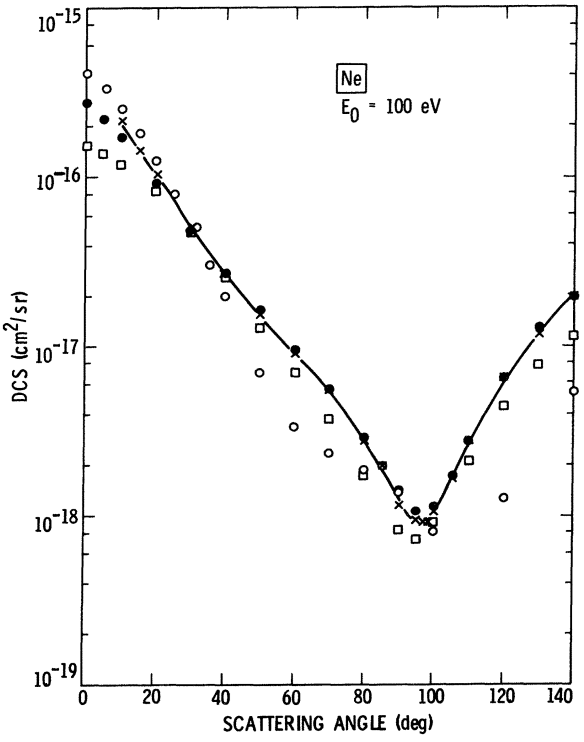

FIG. 6. Comparison of present results with theoretical elastic differential cross sections at 100 eV: ○, Ref. 25; ●, Ref. 3; □, Ref. 4; ×, present (connected by solid line).

the comparison is done with their SEPnaA$_1$ model potential calculation.) The calculation of Byron and Jochain[25] agrees with experiment at low angles but differs significantly (by a factor of 2) at high angles. Figure 7 shows the general trend in the DCS curves with impact energy.

C. Critical minimum

The critical minimum in neon has been the subject of some controversy since the experimental study of Kollath and Lucas[13] located this feature at a point (74 eV, 102°) in disagreement with almost all available theories. Fon and Berrington's recent R-matrix calculations[3] cite this discrepancy as possibly arising from the lack of spin-orbit coupling effects in their studies. Since the experimental data of Kollath and Lucas required a 7-eV correction to the energy scale (due to contact potentials) it was deemed advisable to reinvestigate this phenomenon.

Elastic differential cross sections at 50, 60, 65, 70, and 80 eV were analyzed for the behavior of the critical minimum. The minimum DCS was plotted against energy and against scattering angle. An interpolation of the energy plot was used to fix the critical energy and the uncertainty in the energy location was used to evaluate the error limits on the critical angle. The result of this analysis indicates a critical energy of 62.5±2.5 eV and a critical angle of 101.5°±1.5°. The critical angle reported here is consistent with the earlier experimental results but the present critical energy is substantially lower. Although the statistical uncertainties in the minimum DCS are quite large (due to the very low electron count rates at the minimum), the results of this study are completely inconsistent with an energy location below 60 eV or above 65 eV.

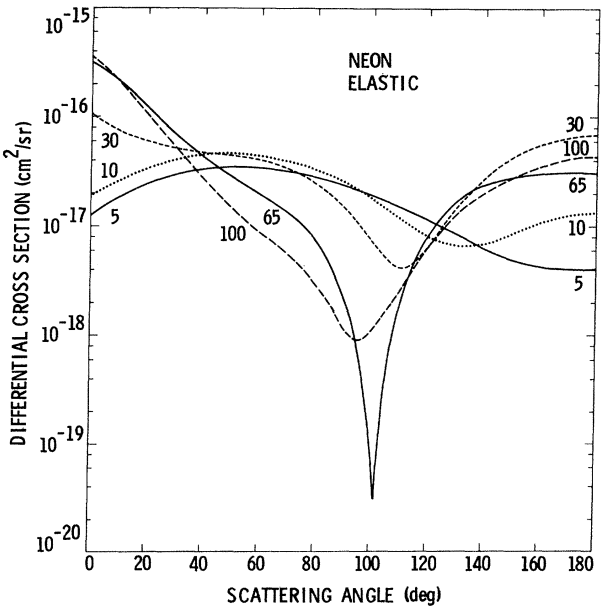

FIG. 7. A comparison of the DCS curves at various impact energies. The low-angle extrapolation is based on the phase-shift values while the high-angle extrapolation is based on phase-shift values and theoretical results of Fon *et al.* (Ref. 3).

Comparison with the DCS recently reported by Menandez *et al.*[14] in this energy range is made in Fig. 8. Although their absolute scale appears to be ~20% higher (resulting from their phase-shift normalization above threshold), the overall shape is in excellent agreement with our data. In particular, the difference in angular position of the minimum is less than 1°. The present results are entirely consistent with their location (64 eV, 102°) and both data are in very good agreement with the most recent theoretical calculations. (See Table VI.) Thus, spin-orbit effects in calculations for the critical minimum in Ne seem to be of little importance.

D. Integral and momentum-transfer cross sections

Table III (in column 2) contains the integral elastic-scattering cross sections derived by our semiempirical procedures and used for normalizing our measurements. For comparison the integral elastic cross sections obtained from the phase-shift fitting of the experimental intensity distributions (without any constraint) are also given (column 3) in the same table. The agreement between the two columns is excellent in the 15- to 30-eV range. Here the DCS curves have prominent structures and the fit becomes more unique and inelastic scattering is absent or small compared to elastic scattering. At 5 and 10 eV the phase shift fit has a few percent uncertainty due to the structureless nature of the intensity distribution and this causes the order of 10% deviation. As the impact energy is increased the deviation between the two columns becomes significant. The effect of the inelastic channels is clearly demonstrated. It is interesting to note that at around 60 eV the deviations reach their maximum value indicating the strongest influence by one- and two-electron excitation and ionization processes. At higher impact energies the deviation becomes smaller again.

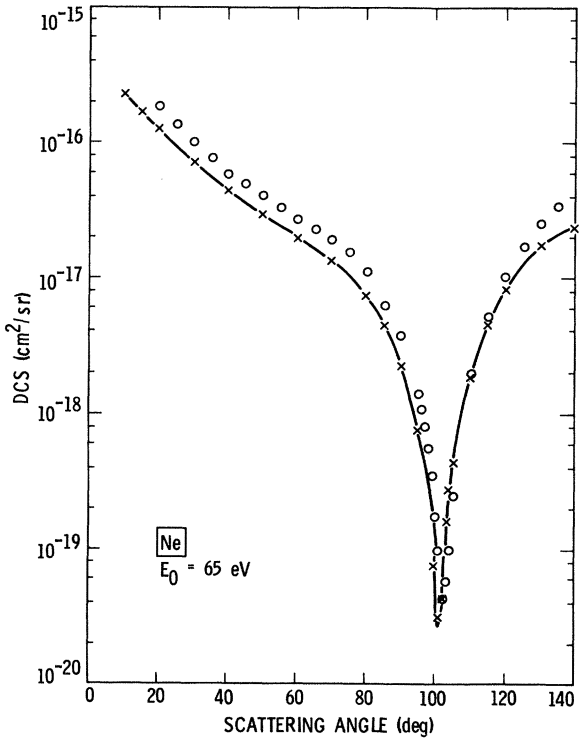

FIG. 8. Elastic differential cross sections near the critical energy: ○, Ref. 14 at 64 eV; ×, present (connected by soild line).

TABLE VI. Critical energy and angle for Ne.

Reference	E_0 (eV)	θ (deg)
Kollath-Lucas (1979)	73.7	103.0
Menandez *et al.* (1980)	64	102
Present	62.5±2.5	101.7±1.5

The results of recent calculations[3,4] are shown for the purpose of comparison in Table III. The R-matrix calculations of Fon and Berrington are in excellent agreement with the present integral cross sections. The agreement with the model potential calculation of Thirumalai and Truhlar are also impressive but not as good as in the case of the R-matrix results.

The momentum-transfer cross sections obtained from the present DCS are summarized in Table VII and shown in Fig. 9. There is an excellent agreement among the various results except at energies above 30 eV where the results of Thirumalai and Truhlar are lower than the other data. The small dip in the present data at around 65 eV coincides with the critical energy and should be due to the deep minimum in the DCS. The theoretical results of Fon and Berrington do not show this dip. The momentum-transfer cross-section values given by Gupta and Rees[10] have been corrected as suggested by Thirumalai and Truhlar.[4]

E. Error estimation

Since the integral elastic cross sections are derived from the total, ionization and excitation cross sections available in the literature, the present normalization is sensitive to the errors associated with these data. The largest contribution at all energies arises from the total cross section which is believed accurate to 3% throughout the energy

TABLE VII. Momentum-transfer cross sections (10^{-16} cm^2) for Ne. Estimated errors are given in square brackets.

		Theory	
		Fon-Berrington	Thirumalai-Truhlar
E_0 (eV)	Present	Ref. 3	Ref. 4
5	1.99 [10]	1.93	
10	2.26 [10]	2.22	2.57
15	2.61 [10]		
20	2.80 [10]	3.04	
30	2.95 [10]	3.11	2.78
40		2.82	
50	2.40 [12]	2.59	2.05
60	1.73 [15]	2.27	
65	1.55 [15]		
70	1.66 [15]	2.08	
80	1.71 [15]		
90			
100	1.32 [15]	1.55	0.94

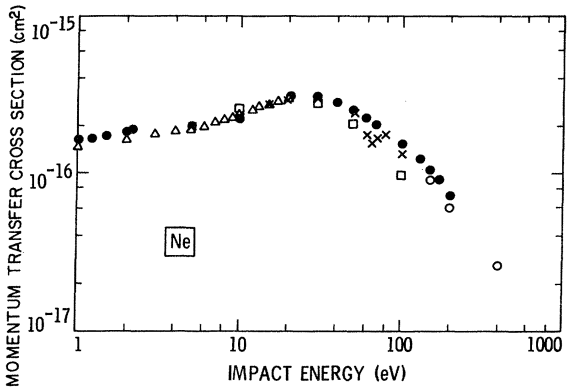

FIG. 9. Momentum-transfer cross sections: ●, Ref. 1 (below 2.2 eV); ●, Ref. 3 (above 5 eV); △, Ref. 9; ○, Ref. 10 (as corrected in Ref. 4); □, Ref. 4; ×, present.

range covered here. Above 30-eV significant contributions arise from ionization and excitation processes which have been summarized in Table II.

The errors associated with the ionization data of Rapp and Englander-Golden is approximately 7% for Ne while the de Heer *et al.* semiempirical estimates range from 3% to 10%. The average value for Q_{ION} given in the third column of Table II may thus represent a worst case accuracy of about 10% which is consistent with the general agreement between the two data sets. The excitation cross sections also semiempirically estimated by de Heer *et al.* are claimed to possess an accuracy of approximately 20%. Unfortunately, it is difficult to assess this data. At two energies, however, Register *et al.*[20] have estimated a lower bound to Q_{EXC} by summing the integral cross sections for the first 40 features in Ne. These latter values are 77% and 29% larger than the de Heer *et al.* data at 30 and 50 eV, respectively. The value given by Register *et al.* at 100 eV represent the sum of only the two strongest transitions in Ne and is given only for comparative purposes.

For the present purposes, both Q_{ION} and Q_{EXC} contribute no more than 20% to Q_{TOT} so that relatively larger errors in these quantities have a relatively small effect on Q_{ELAS}. These errors, properly weighted for the relative cross-section contributions, are given in Table III. The actual estimated errors in the DCS values are given as the last entry in each column of Table V. These errors are larger than those for Q_{ELAS} since the normalization of the DCS relies on an extrapolation of the measured angular distribution (via the phase-shift analysis) to experimentally inaccessible angles (0° and 180°). The errors in the DCS arising from this extrapolation are estimated to vary from 3% to 5%. The momentum-transfer cross sections (Table VII) are derived from the normalized DCS and have relatively larger errors since the momentum-transfer integration depends more heavily on the large angle DCS extrapolation.

ACKNOWLEDGMENTS

We would like to express our gratitude to D. Andrick, W. Wilson, D. Thirumalai, D. G. Truhlar, E. C. Beaty, J. A. Rees, and M. J. Menandez for making their data available to us prior to publication, and to D. G. Truhlar for valuable discussions. The research described in this paper was performed at the Jet Propulsion Laboratory, California Institute of Technology under contract with the National Aeronautics and Space Administration.

[1]T. F. O'Malley and R. W. Crompton, J. Phys. B 13, 3451 (1980).
[2]F. J. de Heer, R. H. J. Jansen, and W. van der Kaay, J. Phys. B 12, 979 (1979).
[3]W. C. Fon and K. A. Berrington, J. Phys. B 14, 323 (1981).
[4]D. Thirumalai and D. G. Truhlar, Phys. Rev. A 25, 3058 (1982); 26, 793 (1982).
[5]R. W. Wagenaar and F. J. de Heer, J. Phys. B 13, 3855 (1980).
[6]W. E. Kauppila, T. S. Stein, J. H. Smart, M. S. Dababneh, Y. K. Ho, J. P. Downing, and V. Pol, Phys. Rev. A 24, 725 (1981).
[7]J. C. Nickel, D. F. Register, and S. Trajmar, in *Abstracts of the XII International Conference on the Physics of Electronic and Atomic Collisions, Gatlinburg, Tennessee, 1981,* edited by S. Datz (North-Holland, Amsterdam, 1981), p. 116.
[8]W. Wilson (unpublished), private communication.
[9]D. Andrick (unpublished), private communication.
[10]S. C. Gupta and J. A. Rees, J. Phys. B 8, 417 (1975); 8, 1267 (1975).
[11]J. F. Williams, J. Phys. B 12, 265 (1979).
[12]D. F. C. Brewer, W. R. Newell, S. F. W. Harper, and A. C. H. Smith, J. Phys. B 14, L749 (1981).
[13]K. J. Kollath and C. J. Lucas, Z. Phys. A 292, 215 (1979).
[14]M. J. Menandez, J. A. Rees, and E. C. Beaty, in *Proceedings of the Thirty-Third Gaseous Electronics Conference, Norman, OK, October, 1980* and private communication (unpublished).
[15]S. P. Khare and D. Raj, J. Phys. B 13, 4627 (1980).
[16]D. F. Register, S. Trajmar, and S. K. Srivastava, Phys. Rev. A 21, 1134 (1980).
[17]R. T. Brinkmann and S. Trajmar, J. Phys. E 14, 245 (1981).
[18]D. Rapp and P. J. Englander-Golden, J. Chem. Phys. 43, 1464 (1965).
[19]M. Schaper and H. Scheibner, Beitr. Plasmaphys. 9, 45 (1969).
[20]D. F. Register, S. Trajmar, G. Steffensen, and D. C. Cartwright, following paper, Phys. Rev. A 29, xxx (1984).
[21]J. F. Williams and A. Crowe, J. Phys. B 8, 2233 (1975).
[22]M. V. Kurepa, L. D. Vuskovic, and S. D. Klalezic, in Abstacts of Papers, *Proceedings of the Eighth International Conference on the Physics of Electronic and Atomic Collisions, Belgrade, Yugoslavia,* edited by B. C. Čorbic and M. V. Kurepa (Institute of Physics, Belgrade, Yugoslavia, 1973), pp. 267–268.
[23]R. H. J. Jansen, F. J. de Heer, H. J. Luyken, B. van Wingerden, and H. J. Blaauw, J. Phys. B 9, 185 (1976).
[24]R. D. DeBois and M. E. Rudd, J. Phys. B 9, 2657 (1976).
[25]F. W. Byron, Jr. and C. J. Joachin, Phys. Rev. A 15, 128 (1977).